

A PLANE THEORY OF INEXTENSIBLE TRANSVERSELY ISOTROPIC ELASTIC COMPOSITES†

L. W. MORLAND‡

Department of Applied Mechanics and Engineering Sciences,
University of California, San Diego, La Jolla, California 92037

Abstract—A plane strain or plane stress configuration of an inextensible transversely isotropic linear elastic material, with the axis of symmetry in the plane, leads to a harmonic lateral displacement field in stretched coordinates. Various displacement and traction conditions lead to standard and nonstandard boundary value problems of potential theory. Examples for a rectangular plane, half-plane and infinite plate with elliptic hole, are presented in illustration.

1. INTRODUCTION

THE MOST simple, yet practically important, type of fibre-reinforced composite consists of an elastic matrix in which are embedded approximately parallel fibres. When the fibres are randomly located in the transverse cross-section, and at sufficient density, the composite body is in some mean sense homogeneous and transversely isotropic about the fibre direction. If the fibres also are elastic, then over stress ranges in which bonding remains essentially intact, the composite material is elastic, and for some stress range undergoes only infinitesimal strain. The mean response of the composite is then represented by the response of a transversely isotropic linear elastic body; see, for example, the review article by Hashin [1]. This description cannot predict stress partition between fibre and matrix, and in particular the local conditions at interfaces, but will reveal regions of high mean stress concentration where further structural support may be required.

A common feature of fibre-reinforced composites is their relatively high modulus of extension in the fibre direction. Rogers and Pipkin [2] point out that this property allows a simplifying approximation to the generally complex stress analysis of transversely isotropic elastic bodies. They introduce an idealized theory in which the composite is assumed to be inextensible in the fibre direction and also incompressible, and consider plane strain in a plane parallel to the fibres. Incompressibility then implies inextensibility in the direction normal to the fibres also, and the permitted displacement field takes a very simple form. This idealized theory (henceforth referred to as IDT) is illustrated by treating the deflection of a rectangular slab with fibres parallel to the axis, with one end fixed and subject to normal side load and shear end load. The interesting predictions of IDT are that deformation takes place by shear in contrast to classical bending theory, as the "fixed-end" condition "penetrates" down the slab, and that infinite tensile (compressive) stress con-

† This research was supported by the National Science Foundation under Grant NSF GK-34017.

‡ Visiting Professor, on leave from School of Mathematics and Physics, University of East Anglia, Norwich, England.

centrations arise at boundaries parallel and normal to fibres to balance applied shear tractions. The interior shear-stress is restricted by the simple form of permitted displacement field while the arbitrary inextensibility and incompressibility constraint stresses depend only on equilibrium and boundary conditions. Spencer [3] shows that the same elementary kinematics of IDT allow a plane strain bending solution of a laminated plate in which the fibres are oblique to the plane of bending.

An interpretation and justification of these unusual predictions of IDT—surface layers of infinite stress and stress penetration down fibres and normal lines—is provided by Everstine and Pipkin [4]. The Airy stress function for plane strain of a transversely isotropic elastic body, with the axis of symmetry in the plane, satisfies an elliptic fourth-order equation in which the five elastic constants appear only in the form of two dimensionless parameters ε_t and ε_c . Inextensibility is the limit $\varepsilon_t \rightarrow 0$, and incompressibility is the limit $\varepsilon_c \rightarrow 0$ subject to an inequality between ε_t and ε_c . Some elementary exact solutions for a half-plane with fibres parallel or normal to the boundary, subjected to sinusoidal loads, are obtained. Leading terms for small ε_t and ε_c reveal the boundary layers of high stress gradient and stress penetration over a large depth, with estimates of both length scales, and demonstrate how the corresponding IDT solutions approximate these features. Setting $\varepsilon_t = \varepsilon_c = 0$ leads to a hyperbolic equation for the stress function and IDT becomes a part of a singular perturbation approach for small $\varepsilon_t, \varepsilon_c$.

While the “nearly inextensible” approximation $\varepsilon_t \sim 0$ is good in many cases, the “nearly incompressible” approximation $\varepsilon_c \sim 0$ does not appear to be so commonly applicable. Furthermore, in a plane stress theory appropriate for plates, the parameter analogous to ε_t is not small, even in the incompressible limit. In these cases an approximate theory assuming only inextensibility $\varepsilon_t = 0$ is more relevant, and provides the appropriate simplification to the full transverse isotropy plane theory. Singular stress layers can still occur at boundaries parallel to fibres, showing the boundary layer present in an exact solution, and hence pointing to difficulties which may be encountered in a direct numerical treatment of the exact equations.

This paper develops the plane theory for an inextensible transversely isotropic elastic material in infinitesimal strain (henceforth described as IT). As in IDT the longitudinal displacement, parallel to the fibres, depends only on the transverse coordinate, but the transverse displacement is harmonic in (finitely) stretched coordinates. Traction conditions on boundaries parallel to fibres lead to a simple normal derivative prescription unaffected by any singular layer associated with the shear traction, while on nonparallel boundaries displacement and traction conditions lead to various boundary-value problems of potential theory, with one class of nonstandard form. Some closed-form solutions can be derived but, more important, there are well established finite-element procedures available for numerical computation of the standard problems, and modification for the nonstandard class appears feasible. Furthermore, any boundary layer effect is not present in this potential part of the solution.

The theory is illustrated in a number of ways. A comparison with the exact half-plane solutions given in [4], and corresponding IDT solutions, is made for $\varepsilon_t \sim 0$. Two rectangular slab (plate) shearing problems are solved numerically, for fibres parallel to the sides, and compared with IDT solutions, including a case of small ε_c . An infinite plate containing an elliptic hole is treated by conformal mapping, and solutions are presented for uniform pressure loading of the hole boundary and for uniform transverse tension at infinity.

2. TRANSVERSE ISOTROPY, INEXTENSIBILITY AND PLANE THEORY

Referred to rectangular Cartesian axes $Ox_1x_2x_3$ with Ox_1 the preferred (fibre) direction, the elastic stress-strain laws for transverse isotropy [1, 4, 5] have the two convenient forms

$$\begin{aligned}\sigma_{11} &= (E_L + 4\nu_L^2 k_T)e_{11} + 2\nu_L k_T e_{\gamma\gamma}, \\ \sigma_{1\alpha} &= 2\mu_L e_{1\alpha}, \\ \sigma_{\alpha\beta} &= 2\mu_T e_{\alpha\beta} + \{(k_T - \mu_T)e_{\gamma\gamma} + 2\nu_L k_T e_{11}\}\delta_{\alpha\beta};\end{aligned}\tag{2.1}$$

and

$$\begin{aligned}E_L e_{11} &= \sigma_{11} - \nu_L \sigma_{\gamma\gamma}, & 2\mu_L e_{1\alpha} &= \sigma_{1\alpha}, \\ e_{\alpha\beta} &= \frac{\sigma_{\alpha\beta}}{2\mu_T} - \left(\frac{\nu_T}{E_T} \sigma_{\gamma\gamma} + \frac{\nu_L}{E_L} \sigma_{11} \right) \delta_{\alpha\beta};\end{aligned}\tag{2.2}$$

where

$$\frac{\nu_T}{E_T} = \frac{E_L(k_T - \mu_T) - 4\nu_L^2 k_T \mu_T}{4E_L k_T \mu_T}.\tag{2.3}$$

Greek subscripts take the values 2, 3, and a repeated index implies summation over those values. E_L , ν_L and E_T , ν_T are the Young's modulus and Poisson's ratio for simple tension in the longitudinal (fibre) direction and in a transverse direction respectively. μ_L , μ_T are the shear moduli for simple shear in the x_1 -direction and in the transverse plane Ox_2x_3 , respectively. k_T is the bulk modulus for plane strain in the transverse plane. Various other sets of 5 independent elastic constants may be chosen [5]. Positive strain energy requires

$$E_L > 0, \quad \mu_L > 0, \quad \mu_T > 0, \quad k_T > 0.\tag{2.4}$$

Low extensibility in the fibre direction may be defined by the strong inequality $E_L \gg \mu_L$; that is,

$$\varepsilon^2 = \frac{\mu_L}{E_L} \ll 1,\tag{2.5}$$

while μ_T , k_T , E_T are of order μ_L . ε is a first-order approximation to the small parameter ε_i introduced in [4]. In the inextensible idealization $\varepsilon = 0$ the first of (2.1) is replaced by

$$e_{11} \equiv 0, \quad \sigma_{11} \text{ arbitrary},\tag{2.6}$$

where the arbitrary workless constraint stress σ_{11} is governed solely by equilibrium and boundary conditions.

First consider plane strain

$$e_{33} = e_{23} = e_{13} = 0, \quad \sigma_{23} = \sigma_{13} = 0,\tag{2.7}$$

with the fibres parallel to the plane. For small ε defined by (2.5), neglecting terms of $O(\varepsilon^2)$ compared with unity and assuming that σ_{11} is not of greater magnitude than all other stress components (2.1)–(2.3) give the approximate relations

$$\begin{aligned}(k_T + \mu_T)\sigma_{33} &= (k_T - \mu_T)\sigma_{22}, & (k_T + \mu_T)e_{22} &= \sigma_{22}, \\ 2\mu_2 e_{12} &= \sigma_{12}, & \mu_L(k_T + \mu_T)e_{11} &= \varepsilon^2 \{(k_T + \mu_T)\sigma_{11} - 2\nu_L k_T \sigma_{22}\}.\end{aligned}\tag{2.8}$$

For equilibrium in the absence of body force the in-plane stress components are given in terms of the Airy stress function $\chi(x_1, x_2)$ by

$$\sigma_{11} = \chi_{,22}, \quad \sigma_{12} = -\chi_{,12}, \quad \sigma_{22} = \chi_{,11}, \quad (2.9)$$

where $,i$ denotes partial differentiation with respect to x_i ($i = 1, 2$). Strain compatibility

$$e_{11,22} + e_{22,11} - 2e_{12,12} = 0, \quad (2.10)$$

implies to the same approximation that

$$\varepsilon^2 \chi_{,2222} + \chi_{,1212} + c^2 \chi_{,1111} = 0, \quad (2.11)$$

or equivalently,

$$\left(\varepsilon^2 \frac{\partial^2}{\partial x_2^2} + \frac{\partial^2}{\partial x_1^2} \right) \left(\frac{\partial^2}{\partial x_2^2} + c^2 \frac{\partial^2}{\partial x_1^2} \right) \chi = 0, \quad (2.12)$$

where

$$c^2 = \frac{\mu_L}{k_T + \mu_T}. \quad (2.13)$$

The exact stress function equation is given in [4], but is there applied to the case of low extensibility $\varepsilon_t = \varepsilon \sim 0$, together with low compressibility $\mu_L/k_T \sim 0$, when c reduces to a second small parameter ε_c . IDT is the limit $\varepsilon_t = \varepsilon_c = 0$ when (2.6), (2.7) and (2.1) imply

$$u_1 = u_1(x_2), \quad u_2 = u_2(x_1), \quad \sigma_{12} = \mu_L \{u_1'(x_2) + u_2'(x_1)\}, \quad (2.14)$$

and σ_{22} is also an arbitrary constraint stress. The limit $\varepsilon = c = 0$ is not a valid approximation to small ε, c in (2.12) whenever the various gradients cause the ε and c terms to have the same magnitude as the other terms. This situation is demonstrated by the boundary layer and stress penetration effects in the solutions presented in [4].

Complete measurements of all five elastic constants of fibre-reinforced materials do not appear to be available, but there is no evidence to suggest μ_L/k_T is small for typical carbon-epoxy, boron-epoxy systems. Heaton [6] calculates values for fibres arranged in square arrays at different volume concentrations, and for a boron-epoxy composite with fibre volume fraction in the range 0.4–0.7, the parameter c takes values 0.53–0.6 while ε takes values 0.13–0.17.

For plane stress,

$$\sigma_{33} = \sigma_{23} = \sigma_{13} = 0, \quad e_{22} = e_{13} = 0, \quad (2.15)$$

and to the first approximation for small ε , (2.2), (2.3) give

$$4\mu_T k_T e_{33} = -(k_T - \mu_T) \sigma_{22}, \quad 4\mu_T k_T e_{22} = (k_T + \mu_T) \sigma_{22}, \\ 2\mu_L e_{12} = \sigma_{12}, \quad \mu_L e_{11} = \varepsilon^2 (\sigma_{11} - \nu_L \sigma_{22}). \quad (2.16)$$

Equilibrium and compatibility again require (2.9)–(2.12) with c replaced by \bar{c} defined by

$$\bar{c}^2 = \frac{\mu_L(k_T + \mu_T)}{4\mu_T k_T}. \quad (2.17)$$

Even in the incompressible limit $\mu_L/k_T \rightarrow 0$, $\bar{c} \not\rightarrow 0$, and in fact, for $\mu_L \geq \mu_T$, $\bar{c} \geq 0.5$ and increases as μ_L/k_T increases from zero. The range of \bar{c} values from [6] is 0.64–0.67.

Thus, for both plane strain and plane stress, the stress function equation (2.12) with ϵ small and c finite, typically in the range 0.5–1.0, would appear to be a commonly applicable approximation. The corresponding inextensible limit $\epsilon = 0$ (IT) replaces the last of (2.8) and of (2.16) by (2.6). The displacement field then takes the form

$$u_1 = u_1(x_2), \quad u_2 = u_2(x_1, x_2), \tag{2.18}$$

with u_3 zero in plane strain and determined by the first of (2.16) in plane stress. Directly from the stress–strain relations (2.8) or (2.16), the x_2 -component of equilibrium balance implies that

$$c^2 \frac{\partial^2 u_2}{\partial x_1^2} + \frac{\partial^2 u_2}{\partial x_2^2} = 0, \tag{2.19}$$

with c replaced by \bar{c} in plane stress, while, with (2.6), the x_1 -component implies that

$$\sigma_{11} = \mu_L t(x_2) - \mu_L \left\{ u_1''(x_2)x_1 + \frac{\partial u_2}{\partial x_2} \right\}. \tag{2.20}$$

Here $t(x_2)$ is an arbitrary function depending only on boundary conditions, and (2.20) assumes that stress gradients are continuously bounded. The equivalent stress function representation is

$$\begin{aligned} \chi &= \chi_0(x_1, x_2) - \mu_L x_1 u_1(x_2) + f(x_2), & \delta f''(x_2) &= \mu_L t(x_2), \\ c^2 \frac{\partial^2 \chi_0}{\partial x_1^2} + \frac{\partial^2 \chi_0}{\partial x_2^2} &= 0, & \mu_L u_2 &= -\delta \frac{\partial \chi_0}{\partial x_2}, \end{aligned} \tag{2.21}$$

but direct solution of (2.19) is more convenient. In IDT, (2.19) and (2.20) are replaced by

$$\sigma_{22} = \mu_L \{ p(x_1) - u_2''(x_1)x_2 \}, \quad \sigma_{11} = \mu_L \{ t(x_2) - u_1''(x_2)x_1 \}, \tag{2.22}$$

where $p(x_1)$ is an arbitrary function depending only on boundary conditions.

Prescribed displacements on the boundary must be compatible with the first of (2.18), and if not then inextensibility is not satisfied so that large stress gradients arise and the ϵ term in (2.12) is not negligible. It is shown in Section 5 that prescribed tractions on boundaries not parallel to fibres are compatible, but on boundaries $x_2 = \text{constant}$ the functions $u_1(x_2)$ and $t(x_2)$ are constant, and σ_{12} , σ_{22} may not both be prescribed compatible with a solution of (2.19). The resulting shear-stress discontinuities and balancing infinite fibre-stress gradient, as predicted along fibre and normal line boundaries in IDT, are approximations to boundary layers of high stress gradient as demonstrated by the solutions in [4]. In an infinitesimal layer at a boundary $x_2 = \text{const}$, equilibrium requires that

$$\frac{\partial \Sigma_{11}}{\partial x_1} + [\sigma_{12}] = 0, \tag{2.23}$$

where

$$\delta \sigma_{11} \rightarrow \Sigma_{11} \text{ (finite) as } \delta \rightarrow 0. \tag{2.24}$$

Thus, the applied shear traction $\tau(x_1)$ may be discontinuous with the interior shear-stress σ_{12} provided that the jump $[\sigma_{12}]$ is balanced by a concentrated fibre stress gradient as in (2.23). The representation (2.20) applies only in the continuous interior solution.

Some half-plane and rectangular plate examples are presented in the next two sections and compared with IDT. In Section 5, the potential theory for (2.19) in stretched coordinates is described for various classes of boundary conditions, and an infinite plate with elliptic hole example is treated in the final section.

3. HALF-PLANE EXAMPLES

The notation $x_1 = x$, $x_2 = y$, $u_1 = u$, $u_2 = v$, etc., will henceforth be adopted for convenience. Solutions to four half-plane examples given by the present inextensible theory IT, (2.8), (2.18), (2.19), (2.20) and (2.23), can be compared with the leading terms for small ε of the exact solutions presented in [4], and with the IDT solutions of (2.14), (2.22).

First consider the half-plane $y \geq 0$ with fibres parallel to the boundary. For the boundary condition

$$y = 0: \sigma_{xy} = \sigma_o \cos\left(\frac{x}{L}\right), \quad \sigma_{yy} = 0, \quad (3.1)$$

with σ_{xx} vanishing as $x \rightarrow \pm\infty$ ($y > 0$) and u, v bounded at infinity, both IT and IDT give for $y > 0$,

$$u = v = 0, \quad \sigma_{xx} = \sigma_{yy} = \sigma_{xy} = 0, \quad (3.2)$$

while the exact solution gives for small ε (finite c),

$$\begin{aligned} \sigma_{xx} &= \frac{\sigma_o}{\varepsilon} \exp\left(-\frac{y}{L\varepsilon}\right) \sin\left(\frac{x}{L}\right) + O(\varepsilon), \\ \sigma_{yy} &= O(\varepsilon), \quad \sigma_{xy} = \sigma_o \exp\left(\frac{-y}{L\varepsilon}\right) \cos\left(\frac{x}{L}\right) + O(\varepsilon). \end{aligned} \quad (3.3)$$

Thus there is a boundary layer of thickness $L\varepsilon$ in which the applied shear stress decays rapidly and in which there is a concentrated tensile stress σ_{xx} represented in IT by (2.23) and (2.24). For the boundary condition

$$y = 0: \sigma_{xy} = 0, \quad \sigma_{yy} = -\sigma_o \cos\left(\frac{x}{L}\right), \quad (3.4)$$

with σ_{xx} vanishing as $x \rightarrow \pm\infty$ ($y > 0$) and u, v bounded at infinity. IT gives for $y > 0$,

$$\begin{aligned} u &= 0, \quad v = \frac{c\sigma_o L}{\mu_L} \exp\left(\frac{-cy}{L}\right) \cos\left(\frac{x}{L}\right), \\ \sigma_{xx} &= c^2 \sigma_o \exp\left(\frac{-cy}{L}\right) \cos\left(\frac{x}{L}\right), \quad \sigma_{yy} = -\sigma_o \exp\left(\frac{-cy}{L}\right) \cos\left(\frac{x}{L}\right), \\ \sigma_{xy} &= -c\sigma_o \exp\left(\frac{-cy}{L}\right) \sin\left(\frac{x}{L}\right). \end{aligned} \quad (3.5)$$

IDT gives for $y > 0$,

$$u = v = 0, \quad \sigma_{xx} = \sigma_{xy} = 0, \quad \sigma_{yy} = -\sigma_o \cos\left(\frac{x}{L}\right), \quad (3.6)$$

which are the limits as $c \rightarrow 0$ of (3.5). Leading terms of the exact solution give σ_{yy} as in (3.5), and

$$\begin{aligned} \sigma_{xx} &= \sigma_o \cos\left(\frac{x}{L}\right) \left\{ c^2 \exp\left(\frac{-cy}{L}\right) - \frac{c}{\varepsilon} \exp\left(\frac{-y}{L\varepsilon}\right) \right\}, \\ \sigma_{xy} &= -c\sigma_o \sin\left(\frac{x}{L}\right) \left\{ \exp\left(\frac{-cy}{L}\right) - \exp\left(\frac{-y}{L\varepsilon}\right) \right\}, \end{aligned} \tag{3.7}$$

showing the boundary layer of thickness $L\varepsilon$ with rapidly varying shear-stress and concentrated stress σ_{xx} .

Now consider the half-plane $x \geq 0$ with fibres normal to the boundary. For the boundary condition

$$x = 0: \sigma_{xy} = \sigma_o \cos\left(\frac{y}{L}\right), \quad \sigma_{xx} = 0, \tag{3.8}$$

with u, v, σ_{xx} bounded as $x \rightarrow \infty$, IT gives for $x \geq 0$,

$$\begin{aligned} u &= 0, \quad v = -\frac{c\sigma_o L}{\mu_L} \exp\left(\frac{-x}{cL}\right) \cos\left(\frac{y}{L}\right), \\ \sigma_{xx} &= c\sigma_o \left\{ 1 - \exp\left(\frac{-x}{cL}\right) \right\} \sin\left(\frac{y}{L}\right), \quad \sigma_{yy} = \frac{\sigma_o}{c} \exp\left(\frac{-x}{cL}\right) \sin\left(\frac{y}{L}\right), \\ \sigma_{xy} &= \sigma_o \exp\left(\frac{-x}{cL}\right) \cos\left(\frac{y}{L}\right), \end{aligned} \tag{3.9}$$

and IDT gives for $x > 0$,

$$u = v = 0, \quad \sigma_{xx} = \sigma_{yy} = \sigma_{xy} = 0. \tag{3.10}$$

While (3.9) satisfies both traction conditions (3.8) it implies that σ_{xx} ‘‘penetrates’’ to infinity, $\sim c\sigma_o \sin(y/L)$ as $x \rightarrow \infty$. The exact solution shows, to first-order in ε , that

$$\sigma_{xx} = c\sigma_o \left\{ \exp\left(\frac{-x\varepsilon}{L}\right) - \exp\left(\frac{-x}{cL}\right) \right\} \sin\left(\frac{y}{L}\right), \tag{3.11}$$

so that the actual penetration depth is of order L/ε . For the boundary condition

$$x = 0: \sigma_{xy} = 0, \quad \sigma_{xx} = -\sigma_o \cos\left(\frac{y}{L}\right), \tag{3.12}$$

with u, v, σ_{xx} bounded as $x \rightarrow \infty$. Both IT and IDT give for $x > 0$,

$$u = v = 0, \quad \sigma_{yy} = \sigma_{xy} = 0, \quad \sigma_{xx} = -\sigma_o \cos\left(\frac{y}{L}\right), \tag{3.13}$$

while the exact solution gives

$$\begin{aligned} \sigma_{xy} &= O(\varepsilon), \\ \sigma_{xx} &= \sigma_o \exp\left(\frac{-x\varepsilon}{L}\right) \cos\left(\frac{y}{L}\right) + O(\varepsilon), \\ \sigma_{yy} &= \frac{\sigma_o \varepsilon}{c} \exp\left(\frac{-x}{L\varepsilon}\right) \cos\left(\frac{y}{L}\right) + O(\varepsilon^2), \end{aligned} \tag{3.14}$$

showing the σ_{xx} penetration depth of order L/ε .

4. RECTANGULAR PLATE EXAMPLES

Consider a rectangular plate or slab with cross-section $0 \leq x \leq l$, $0 \leq y \leq h$, so that fibres are parallel to the side Ox , subject to plane strain or plane stress loading. Let one end be fixed and the other end subjected to shear traction only; thus,

$$x = 0: u = v = 0; \quad x = l: \sigma_{xx} = 0, \quad \sigma_{xy} = -\tau(y). \quad (4.1)$$

It follows from the first of (4.1) that in both IT and IDT,

$$u \equiv 0, \quad (4.2)$$

and hence by the third of (4.1) that

$$\text{IDT: } \sigma_{xx} \equiv \mu_L t(y) \equiv 0; \quad \text{IT: } t(y) = \left(\frac{\partial v}{\partial y} \right)_{x=l}. \quad (4.3)$$

Consider two simple side conditions

$$(a) \quad y = 0: \sigma_{xy} = \sigma_{yy} = 0, \quad y = h: \sigma_{xy} = \sigma_{yy} = 0, \quad (4.4)$$

$$(b) \quad y = 0: \sigma_{xy} = \sigma_{yy} = 0, \quad y = h: u = v = 0.$$

The IDT interior solution of (a) [2] is simply

$$v = -\frac{Fx}{\mu_L h}, \quad \sigma_{xy} = -\frac{F}{h}, \quad \sigma_{xx} = \sigma_{yy} = 0, \quad (4.5)$$

where

$$F = \int_0^h \tau(y) dy. \quad (4.6)$$

The shear-stress jumps on $y = 0, h$ are balanced by concentrated compressive and tensile σ_{xx} respectively, as defined in (2.23), (2.24), and if $\tau(y)$ does not have the uniform distribution F/h then the σ_{xy} jump on $x = l$ is similarly balanced by concentrated σ_{yy} in normal lines. In practice the inextensibility approximation $e_{11} \equiv 0$ (or high modulus E_L) may not be appropriate for large compressive stress in the fibre direction, particularly if the matrix largely supports the compressive stress. For (b) the IDT interior solution is simply

$$v = 0, \quad \sigma_{xy} = \sigma_{xx} = \sigma_{yy} = 0, \quad (4.7)$$

with concentrated σ_{yy} on $x = l$.

In terms of the stretched coordinates

$$X = x, \quad Y = cy, \quad (4.8)$$

the IT displacement v , by (2.19), becomes harmonic:

$$V(X, Y) = v(x, y), \quad \nabla^2 V = \frac{\partial^2 V}{\partial X^2} + \frac{\partial^2 V}{\partial Y^2} = 0. \quad (4.9)$$

From the boundary conditions (4.1), (4.4),

$$X = l: \frac{\partial V}{\partial X} = -\frac{\tau(Y/c)}{\mu_L},$$

(a) $Y = 0, ch: \frac{\partial V}{\partial Y} = 0, \quad [\sigma_{xy}] \neq 0,$ (4.10)

(b) $Y = 0: \frac{\partial V}{\partial Y} = 0, \quad [\sigma_{xy}] \neq 0, \quad Y = ch: V = 0,$

implying boundary layers on $y = 0, h$ for (a) and on $y = 0$ for (b). Note that in IDT (b) there is a boundary layer on $x = l$ associated with normal line stress, but no boundary layer on $y = 0$.

These potential problems have been solved numerically by standard finite element methods† for various values of c and the aspect ratio $a = h/l$. The end tractions for the side conditions (a) and (b) of (4.4), (4.10) are chosen to be respectively

(a) $\tau(y) = \frac{2F}{h^2}y, \quad (b) \tau(y) = \frac{F}{h}.$ (4.11)

As illustration the solutions are presented for the case $a = 1$ (square plate) with $c = 1$ and $c = 0.1$. The small value is chosen to demonstrate the approach to the IDT solutions as $c \rightarrow 0$.

Figure 1 shows the displacement v on $y = 0$ and $y = h$ in problem (a) for $c = 1$ and $c = 0.1$, with the latter not distinguishable from the linear IDT profile (4.5), and on $y = 0$ in problem (b). For the latter the $c = 0.1$ solution differs significantly from the vanishing IDT displacement near the sheared end.

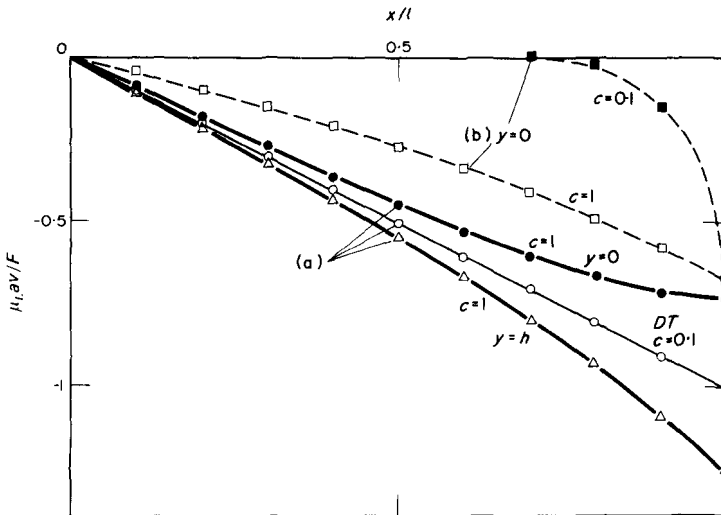


FIG. 1. Transverse displacement for side conditions (a) and (b).

† I am indebted to Dr. M. Baligh of Systems, Science and Software, Inc., for performing the computations.

Figure 2 shows the shear-stress σ_{xy} in problem (a) on $y/h = 0.05$ and 0.95 , for $c = 1$ and $c = 0.1$, and shows the uniform IDT distribution for comparison. The (normal) boundary layer near $x = l$ for $c = 0.1$, approximated by the jump in IDT, is evident. The same comparisons are made in Fig. 3 for problem (b).

Figure 4 shows the transverse stress σ_{yy} on $x/l = 0.95$, near the sheared end, for problem (a), for $c = 1$ and $c = 0.1$. The latter shows the large values of σ_{yy} and $\partial\sigma_{yy}/\partial y$ arising to balance the nonuniform applied shear traction. The same comparisons are made in Fig. 5 for problem (b). Note the higher values of σ_{yy} arising due to the fixed side condition when c is small, but not for $c = 1$.

5. POTENTIAL THEORY

The previous two sections have demonstrated by examples the occurrence of concentrated fibre stress and discontinuous shear-stress at boundaries parallel to fibres when tractions are prescribed. On boundary sections $y = \text{constant}$ the arbitrary functions $u(y)$

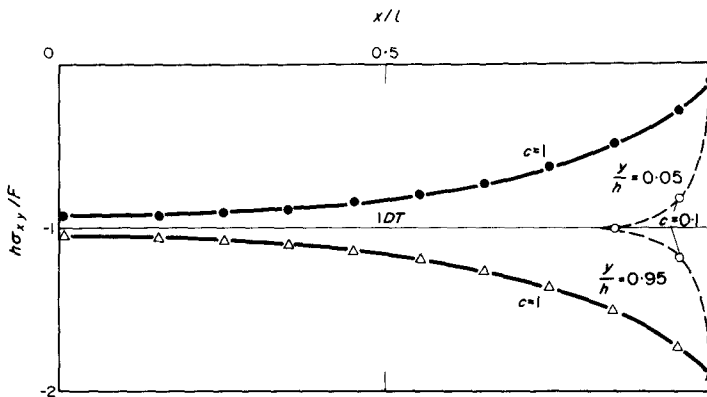


FIG. 2. Shear stress for side conditions (a).

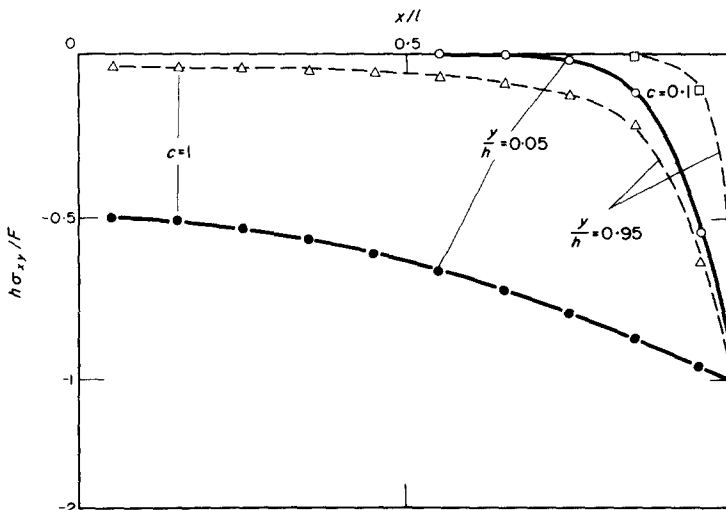


FIG. 3. Shear stress for side conditions (b).

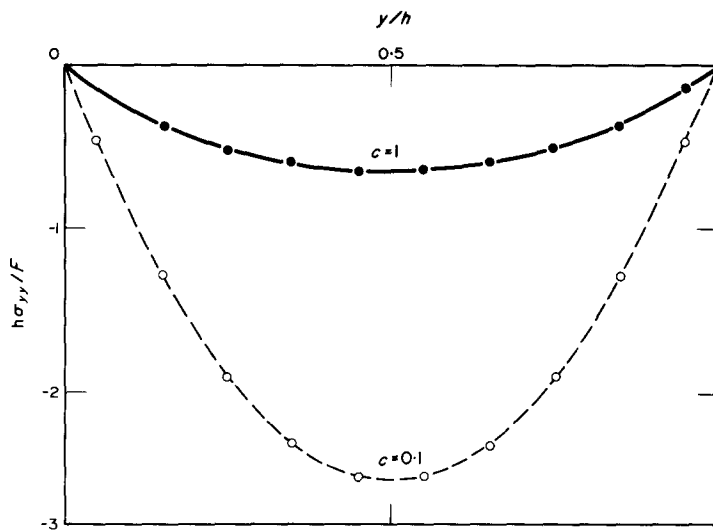


FIG. 4. Transverse stress on $x/l = 0.95$ for side conditions (a).

and $t(y)$ become constants, and two independent traction distributions are an over-prescription (in general) for the elliptic $v(x, y)$ equation (2.19). Similarly, displacement conditions incompatible with a field $u(y)$ will induce high fibre stress in some region and some fibre extension of $O(\epsilon)$, requiring a perturbation approach to a compatible solution.

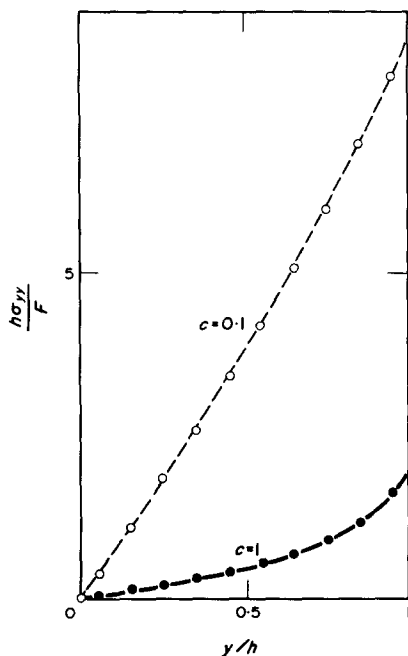


FIG. 5. Transverse stress on $x/l = 0.95$ for side conditions (b).

Domains with boundaries parallel to fibres only at discrete tangent points are now considered. Under the (nonconformal) transformation (4.8) the transverse displacement $v = V(X, Y)$ is harmonic (4.9). Also write

$$U(Y) = u(y), \quad T(Y) = t(y). \tag{5.1}$$

Details are presented for a finite domain D convex to fibre lines $Y = \text{constant}$ as shown in Fig. 6. For boundaries intersecting a section of fibre lines $2r$ times the functions $U(Y)$, $T(Y)$ can be r -valued in that range, continuous with $U(Y)$, $T(Y)$ outside the range. The boundary C of the domain D , Fig. 6, can be divided into left- and right-hand sections, $C = C_L \cup C_R$ where

$$C_L : X = X_L(Y), \quad C_R : X = X_R(Y), \quad Y_0 \leq Y \leq Y_1, \tag{5.2}$$

and X_L is continuous with X_R at Y_0 and Y_1 .

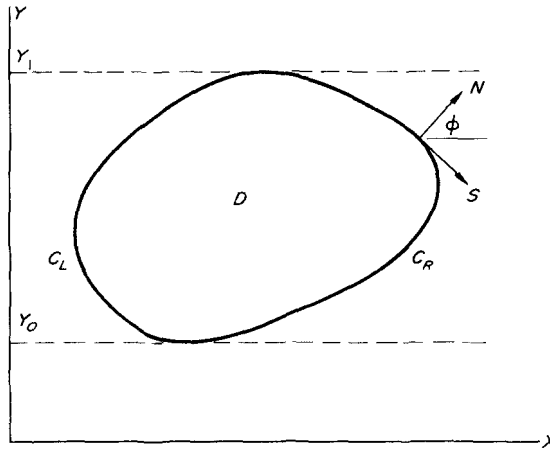


FIG. 6. Body domain in stretched coordinates.

The inclination ϕ of the unit outward normal N on C to the X -axis is related to θ , the inclination of the normal on the body boundary to the x -axis, by

$$\cot \phi = c \cot \theta, \quad \cos \phi = c \cos \theta (c^2 \cos^2 \theta + \sin^2 \theta)^{-\frac{1}{2}}. \tag{5.3}$$

Two useful identities are

$$c^2 \sin^2 \phi \pm \cos^2 \phi = c^2 (\sin^2 \theta \pm \cos^2 \theta) (c^2 \cos^2 \theta + \sin^2 \theta)^{-1}. \tag{5.4}$$

The tractions $\mu_L t_x, \mu_L t_y$ on the body boundary are related to V by

$$\int^s t_x ds = V + cXU'(Y) - c^{-1} \int^Y T(Y) dY, \tag{5.5}$$

$$(c^2 \sin^2 \phi + \cos^2 \phi)^{\frac{1}{2}} t_y = \frac{\partial V}{\partial N} + c \cos \phi U'(Y), \tag{5.6}$$

where s measures arc length (in the sense of S , Fig. 6) along the body boundary. Equivalent to (5.5) is

$$(c^2 \sin^2 \varphi + \cos^2 \varphi)^{\frac{1}{2}} t_x = c \frac{\partial}{\partial S} \{V + cXU'(Y)\} + \cos \varphi T(Y). \tag{5.7}$$

From the self-equilibration of the boundary tractions,

$$\oint_C \frac{\partial V}{\partial S} dS = 0, \quad \oint_C \frac{\partial V}{\partial N} dS = 0, \tag{5.8}$$

as required. The stress components on D are expressed by

$$\begin{aligned} \sigma_{xx} &= \mu_L \left\{ T(Y) - c^2 XU''(Y) - c \frac{\partial V}{\partial Y} \right\}, \\ \sigma_{yy} &= c^{-1} \mu_L \frac{\partial V}{\partial Y}, \quad \sigma_{xy} = \mu_L \left\{ cU'(Y) + \frac{\partial V}{\partial X} \right\}. \end{aligned} \tag{5.9}$$

In view of the functions $U(Y)$, $T(Y)$ uniform in X it is helpful to describe boundary conditions with explicit reference to C_L and C_R . When different conditions are applied on C_L and C_R there is a corresponding problem with C_L and C_R interchanged. Pairing of conditions on C_L and C_R applies also to sub-sections of C_L and C_R over a common range of Y . It is supposed that whenever the displacement u is applied on both C_L and C_R on a common range of Y , it is compatible with the inextensibility requirement $u = U(Y)$. Following is a classification of various prescribed boundary conditions which in principle determine $U(Y)$, $T(Y)$ and harmonic $V(X, Y)$:

$$U \text{ and } V \text{ on } C, \quad t_x \text{ on } C_L, \tag{5.10}$$

$$U \text{ and } t_y \text{ on } C, \quad t_x \text{ on } C_L, \tag{5.11}$$

$$U \text{ on } C, V \text{ on } C_L, \quad t_x \text{ and } t_y \text{ on } C_R, \tag{5.12}$$

$$V \text{ and } t_x \text{ on } C, \tag{5.13}$$

$$t_x \text{ on } C, \quad V \text{ on } C_L, \quad t_y \text{ on } C_R, \tag{5.14}$$

$$t_x \text{ and } t_y \text{ on } C. \tag{5.15}$$

Conditions (5.10)–(5.13) determine the solution V of (4.9) and T is then found from (5.5) for the first three, and U , T are determined by (5.5) given t_x on C_L and C_R (5.13). Given (5.14), V and t_x on C_L relates U and T by (5.5), then t_x on C_R expresses U and T in terms of V on C_R . Consequently, t_y on C_R , by (5.6), prescribes a combination of $\partial V/\partial N$ and V on C_R , and V is given on C_L by (5.14). That is, writing

$$\begin{aligned} \int_{C_L} t_x ds' &= g_L(Y), & \int_{C_R} t_x ds' &= g_R(Y), \\ g_L(Y_0) = g_R(Y_0) &= 0, & g_L(Y_1) = g_R(Y_1) &= g(Y_1), \end{aligned} \tag{5.16}$$

and denoting V on C_L and C_R by $V_L(Y)$, $V_R(Y)$, respectively,

$$\begin{aligned} c\{X_R(Y) - X_L(Y)\}U'(Y) &= g_R(Y) - g_L(Y) - V_R(Y) + V_L(Y), \\ c^{-1}\{X_R(Y) - X_L(Y)\} \int^Y T(Y') dY' &= X_R(Y)\{V_L(Y) - g_L(Y)\} - X_L(Y)\{V_R(Y) - g_R(Y)\}, \end{aligned} \tag{5.17}$$

and hence on C_R , by (5.6),

$$(X_R - X_L) \frac{\partial V}{\partial N} - \cos \varphi V = (X_R - X_L)(c^2 \sin^2 \varphi + \cos^2 \varphi)^{\frac{1}{2}} t_y - \cos \varphi \{g_R - g_L + \bar{V}_L\}, \quad (5.18)$$

where \bar{V}_L denotes V evaluated at the same value of Y on C_L . The conditions (5.10)–(5.14) lead to standard potential problems for V .

Finally, there are the pure traction conditions (5.15). Writing

$$(c^2 \sin^2 \varphi + \cos^2 \varphi)^{\frac{1}{2}} t_y = \begin{cases} f_L(Y) \text{ on } C_L \\ f_R(Y) \text{ on } C_R \end{cases}, \quad (5.19)$$

and denoting φ and $\partial V/\partial N$ on C_L, C_R by $\varphi_L, \partial V_L/\partial N$ and $\varphi_R, \partial V_R/\partial N$, respectively, (5.5) and (5.6) become

$$\left. \begin{aligned} V_Q &= g_Q - c X_Q U' + c^{-1} \int^Y T(Y') dY' \\ \frac{\partial V_Q}{\partial N} &= f_Q - c \cos \varphi_Q U' \end{aligned} \right\} Q = L, R. \quad (5.20)$$

By the first of (5.20) with $Q = L$ and R , the relations (5.17) for U, T are again obtained. Hence, eliminating U' in the second of (5.20),

$$\begin{aligned} C_L: (X_R - X_L) \frac{\partial V}{\partial N} + \cos \varphi (V - \bar{V}_R) &= (X_R - X_L) f_L + \cos \varphi (g_L - g_R), \\ C^R: (X_R - X_L) \frac{\partial V}{\partial N} - \cos \varphi (V - \bar{V}_L) &= (X_R - X_L) f_R + \cos \varphi (g_L - g_R), \end{aligned} \quad (5.21)$$

where \bar{V}_R denotes V evaluated on C_R at the same Y value, and each f_Q, g_Q are evaluated at the current value of Y . Note that $\cos \varphi < 0$ on $C_L, > 0$ on C_R . Equation (5.21) is a non-standard potential problem. At $Y = Y_0$ and Y_1 , $\cos \varphi = 0, X_R = X_L, g_L = g_R$, and (5.21) has continuous limits. It is straightforward to prove the existence of a unique solution V for the boundary conditions (5.18) and (5.21) when C is a circle, but no proof has been found for general C .

The traction problem (5.21) simplifies for boundaries C (and hence the body boundary) symmetric about a normal line, say $X = 0$. Then

$$X_L = -X_R, \quad \cos \varphi_L = -\cos \varphi_R, \quad \sin \varphi_L = \sin \varphi_R. \quad (5.22)$$

Consider the solution as a sum of even and odd parts in $X, V = \overset{\circ}{V} + \overset{\bullet}{V}$. Then $\partial \overset{\circ}{V}/\partial N$ is even and $\partial \overset{\bullet}{V}/\partial N$ is odd. The C_L and C_R conditions for $\overset{\circ}{V}$ are compatible with $f_L = f_R = \overset{\circ}{f}$ (t_y even) and $g_L = g_R = \overset{\circ}{g}$ (t_x odd), that is, symmetric loading, giving on C

$$\frac{\partial \overset{\circ}{V}}{\partial N} = \overset{\circ}{f}, \quad (5.23)$$

a standard potential problem. By (5.17),

$$U'(Y) \equiv 0, \quad \int^Y T(Y') dY' = c \{ \overset{\circ}{V}(Y) - \overset{\circ}{g}(Y) \}, \quad (5.24)$$

$\overset{\circ}{V}$ is the solution for t_y odd, $-f_L = f_R = \overset{\circ}{f}$, and t_x even which implies $g(Y_1) = 0$ (self-equilibration on C_L and C_R separately), and hence $-g_L = g_R = \overset{\circ}{g}$. Thus (5.21) becomes

$$\begin{aligned} C_L: X_R \frac{\partial \overset{\circ}{V}}{\partial N} + \cos \varphi \overset{\circ}{V} &= -X_R \overset{\circ}{f} - \cos \varphi \overset{\circ}{g}, \\ C_R: X_R \frac{\partial \overset{\circ}{V}}{\partial N} - \cos \varphi \overset{\circ}{V} &= X_R \overset{\circ}{f} - \cos \varphi \overset{\circ}{g}, \end{aligned} \tag{5.25}$$

a standard problem, and (5.17) gives

$$cX_R(Y)U'(Y) = \overset{\circ}{g}(Y) - \overset{\circ}{V}_R(Y), \quad T(Y) \equiv 0. \tag{5.26}$$

6. INFINITE PLATE WITH ELLIPTIC HOLE

If the domain D extends to unbounded X then by (5.9) the stress σ_{xx} is bounded only if $U''(Y) \equiv 0: U = U_1 Y$, and if it extends also to unbounded Y then bounded displacement requires $U \equiv 0$. The class of inextensible solutions on infinite domains is therefore restricted, but includes the symmetric traction problems. As illustration, two symmetric loading problems for an infinite plate with an elliptic hole are solved by conformal mapping.

Figure 7 shows an elliptic boundary

$$x = a \cos \omega, \quad y = b \sin \omega, \quad -\pi \leq \omega \leq \pi, \tag{6.1}$$

and the elliptic boundary C under the transformation (4.8):

$$X = A \cos \omega, \quad Y = B \sin \omega, \quad A = a, \quad B = cb. \tag{6.2}$$

Introducing the complex variables $z = X + iY$ and w , the conformal mapping

$$z = \frac{1}{2}(A+B)w + \frac{1}{2}(A-B)w^{-1}, \quad (A+B)w = z + \{z^2 - (A^2 - B^2)\}^{\frac{1}{2}}, \tag{6.3}$$

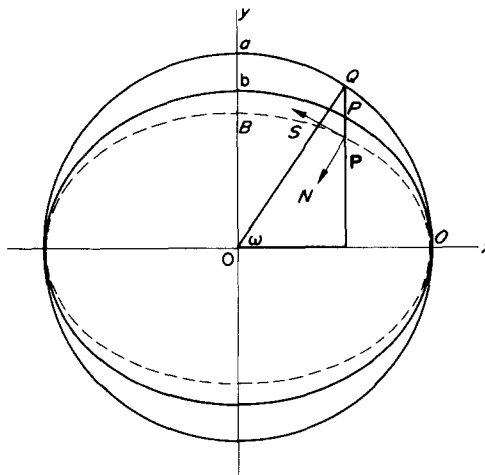


FIG. 7. Elliptic hole boundary and transformation.

maps the exterior D of the ellipse (6.2) onto the exterior of the unit circle $w = e^{i\omega}$. An analytic function $\Omega(z)$ on D maps into an analytic function $\bar{\Omega}(w)$ on $|w| > 1$ and the harmonic function $V(X, Y)$ can be expressed as

$$V(X, Y) = \text{Im}[\Omega(z)] = \text{Im}[\bar{\Omega}(w)]. \tag{6.4}$$

The stress expressions (5.9) can then be written

$$c\sigma_{yy} + i\sigma_{xy} = \mu_L \bar{\Omega}'(w) \frac{dw}{dz}, \quad \sigma_{xx} = \mu_L \left\{ T(Y) - c \text{Re} \left[\bar{\Omega}'(w) \frac{dw}{dz} \right] \right\}, \tag{6.5}$$

in the symmetric case $U \equiv 0$.

On the boundary $w = e^{i\omega}$,

$$\frac{dz}{dw} = e^{-i\omega}(B \cos \omega + iA \sin \omega), \tag{6.6}$$

$$e^{i\varphi} = - \left| \frac{dw}{dz} \right| (B \cos \omega + iA \sin \omega), \tag{6.7}$$

$$\frac{\partial V}{\partial S} - i \frac{\partial V}{\partial N} = \left| \frac{dw}{dz} \right| e^{i\omega} \bar{\Omega}'(e^{i\omega}). \tag{6.8}$$

Here, in the symmetric case $U \equiv 0$, t_x odd, direct from (5.7),

$$B \cos \omega T(B \sin \omega) = t_n B \cos \omega + ct_s A \sin \omega + c \text{Re}[e^{i\omega} \bar{\Omega}'(e^{i\omega})], \tag{6.9}$$

for $-\pi/2 \leq \omega \leq \pi/2$, and the boundary condition (5.22) becomes

$$\text{Im}[e^{i\omega} \bar{\Omega}'(e^{i\omega})] = ct_n A \sin \omega - t_s B \cos \omega, \tag{6.10}$$

on $w = e^{i\omega}$ ($-\pi \leq \omega \leq \pi$), where $\mu_L t_n, \mu_L t_s$ are the normal and tangential tractions on the hole boundary. Here t_n is even, and t_s is odd, in x . Note also that

$$\frac{dz}{dw} \rightarrow \frac{1}{2}(A + B) \quad \text{as } w \rightarrow \infty. \tag{6.11}$$

By (6.9), $T(Y)$ is generally nonzero in $-B \leq Y \leq B$ and so by (6.5) the fibre stress σ_{xx} penetrates to infinity in the $\pm X$ -direction in the ‘‘influence strip’’ of the hole boundary. Requiring $\sigma_{xx} \rightarrow 0$ as $X \rightarrow \pm \infty$ in $|Y| > B$ implies $T(Y) \equiv 0$ in $|Y| > B$ and hence $T(Y), \sigma_{xx}$ may be discontinuous on $Y = \pm B$. Such discontinuities can be regarded as approximations to narrow strips of high σ_{xx} gradient in the y -direction.

Consider first uniform pressure loading of the hole boundary with vanishing shear and transverse stress at infinity:

$$\mu_L t_n = -p, \quad t_s = 0; \quad \sigma_{xy}, \sigma_{yy} \rightarrow 0 \quad \text{as } w \rightarrow \infty. \tag{6.12}$$

The latter imply that $\bar{\Omega}'(w) \rightarrow 0$ as $w \rightarrow \infty$. Assuming a Laurent expansion for $\bar{\Omega}(w)$, (6.10) shows trivially that

$$\bar{\Omega}(w) = -\frac{pcA}{\mu_L w}. \tag{6.13}$$

From (6.9)

$$\mu_L T(B \sin \omega) = -p(1 - c^2 A/B), \quad -\pi/2 \leq \omega \leq \pi/2, \quad (6.14)$$

which is uniform and nonzero, so that stress penetration does occur. The displacement and stresses are obtained from (6.4), (6.5). In particular, on the hole boundary $w = e^{i\omega}$,

$$\mu_L v = pcA \sin \omega = pcya/b, \quad (6.15)$$

$$c\sigma_{yy} + i\sigma_{xy} = \frac{pcA\{B \cos^2 \omega - A \sin^2 \omega - i(A+B) \sin \omega \cos \omega\}}{B^2 \cos^2 \omega + A^2 \sin^2 \omega}, \quad (6.16)$$

$$\sigma_{xx} = -p \left(1 - \frac{c^2 A}{B} \right) - \frac{pc^2 A(B \cos^2 \omega - A \sin^2 \omega)}{B^2 \cos^2 \omega + A^2 \sin^2 \omega}. \quad (6.17)$$

The circumferential stress $\sigma_{ss} = \sigma_{xx} + \sigma_{yy} + p$ becomes

$$\sigma_{ss} = \frac{pA}{B} \left\{ 1 - \frac{A(1 - c^2)(A+B) \sin^2 \omega}{B^2 \cos^2 \omega + A^2 \sin^2 \omega} \right\}. \quad (6.18)$$

For a circular hole $A = 1$, $B = c$ and $0 < c < 1$, σ_{ss} decreases monotonically from $p/c (> 0)$ to $-p(1 - c - c^2) (< 0)$ as ω increases from 0 to $\pi/2$, with symmetric values in the other quadrants. Compare the solution $\sigma_{ss} \equiv p$ for an isotropic plate, obtained here when $c = 1$. For small c , σ_{ss} has a high tensile value at $\omega = 0$ and is compressive at $\omega = \pi/2$, but $\sigma_{ss} \rightarrow -p$ (all $\omega \neq 0, \pi$) as $c \rightarrow 0$, showing the small section of high σ_{ss} gradient near $\omega = 0, \pi$ for small c .

Next consider zero boundary traction and uniform transverse tension at infinity:

$$t_n = t_s = 0; \quad \sigma_{yy} \rightarrow F, \quad \sigma_{xy} \rightarrow 0 \quad \text{as } w \rightarrow \infty. \quad (6.19)$$

For these conditions

$$\bar{\Omega}(w) = \frac{Fc(A+B)}{2\mu_L} \left(w - \frac{1}{w} \right), \quad (6.20)$$

and

$$\mu_L T(B \sin \omega) = Fc^2(1 + A/B), \quad -\pi/2 \leq \omega \leq \pi/2. \quad (6.21)$$

On the hole boundary

$$\mu_L v = Fc(A+B) \sin \omega = Fcy(a+cb)/b, \quad (6.22)$$

$$c\sigma_{yy} + i\sigma_{xy} = \frac{Fc(A+B) \cos \omega (B \cos \omega - iA \sin \omega)}{B^2 \cos^2 \omega + A^2 \sin^2 \omega}, \quad (6.23)$$

$$\sigma_{xx} = \frac{Fc^2(A+B)}{B} - \frac{Fc^2(A+B)B \cos^2 \omega}{B^2 \cos^2 \omega + A^2 \sin^2 \omega}, \quad (6.24)$$

$$\sigma_{ss} = \frac{F(A+B)(B^2 \cos^2 \omega + c^2 A^2 \sin^2 \omega)}{B(B^2 \cos^2 \omega + A^2 \sin^2 \omega)}. \quad (6.25)$$

For the circular hole σ_{ss} decreases from $F(1+c)/c$ to $Fc(1+c)$ as ω increases from 0 to $\pi/2$, when $0 < c < 1$, with symmetric behaviour in the other quadrants. For $c = 1$,

$\sigma_{ss} \equiv 2F$. Compare the maximum tensile value $F(1+c)/c$ at $\omega = 0$ with the isotropic plate result $3F$. As $c \rightarrow 0$ ($\omega \neq 0, \pi$), $\sigma_{ss} \sim Fc \operatorname{cosec}^2 \omega$.

Note

I have recently been shown a manuscript entitled "Plane Strain and Generalised Plane Stress Problems for Fibre-Reinforced Materials" by A. H. England, J. E. Ferrier and J. N. Thomas, Department of Theoretical Mechanics, University of Nottingham, submitted to the *Journal of the Mechanics and Physics of Solids*. The transverse displacement equations (2.19) and (4.9) are derived under the same assumptions, and in illustration some solutions for the infinite plane, half plane, and infinite strip are obtained, and compared with the IDT solutions in the limit $c \rightarrow 0$.

REFERENCES

- [1] Z. HASHIN, Theory of composite materials. In *Mechanics of Composite Materials*. Editors F. W. WENDT, H. LIEBOWITZ and N. PERRONE, pp. 201–242. Pergamon Press (1970).
- [2] T. G. ROGERS and A. C. PIPKIN, Small deflections of fibre-reinforced beams or slabs. *J. appl. Mech.* **38**, 1047–1048 (1971).
- [3] A. J. M. SPENCER, Plane strain bending of laminated fibre-reinforced plates. *Q. J. Mech. Appl. Math.* **25**, 387–400 (1972).
- [4] G. C. EVERSTINE and A. C. PIPKIN, Stress channelling in transversely isotropic elastic composites. *Z. angew. Math. Phys.* **22**, 825–834 (1971).
- [5] S. G. LEKHNITSKII, *Theory of Elasticity of an Anisotropic Elastic Body*. Holden-Day (1963).
- [6] M. D. HEATON, A calculation of the elastic constants of a unidirectional fibre-reinforced composite. *Br. J. appl. Phys.* **1**, 1039–1048 (1968).

(Received 31 January 1973; revised 30 April 1973)

Абстракт—Очертание плоской деформации или плоского напряжения для нерастяжимемого, поперечно изотропного линейного, упругого материала, с осей симметрии в плоскости, приводит к гармонически поперечному полю перемещений в удлиненных координатах. Разные условия перемещений и тяговых усилий сводятся к стандартным и нестандартным краевым задачам теории потенциала. Для иллюстрации, даются примеры для прямоугольной плоскости, полуплоскости и бесконечной пластинки с эллиптическим отверстием.